Biosci. Rep. (2013) / **33** / art:e00021 / doi 10.1042/BSR20120097

Original Paper

OPEN ACCESS

Dihydro-orotate dehydrogenase is physically associated with the respiratory complex and its loss leads to mitochondrial dysfunction

JingXian FANG*†, Takeshi UCHIUMI*[1], Mikako YAGI*, Shinya MATSUMOTO*, Rie AMAMOTO*, Shinya TAKAZAKI*, Haruyoshi YAMAZA†, Kazuaki NONAKA† and Dongchon KANG*

*Department of Clinical Chemistry and Laboratory Medicine, Graduate School of Medical Sciences, Kyushu University, 3-1-1 Maidashi, Higashi-ku, Fukuoka 812-8582, Japan, and †Department of Pediatric Dentistry, Graduate School of Dental Science, Kyushu University, 3-1-1 Maidashi, Higashi-ku, Fukuoka 812-8582, Japan

Synopsis

Some mutations of the *DHODH* (dihydro-orotate dehydrogenase) gene lead to postaxial acrofacial dysostosis or Miller syndrome. Only DHODH is localized at mitochondria among enzymes of the *de novo* pyrimidine biosynthesis pathway. Since the pyrimidine biosynthesis pathway is coupled to the mitochondrial RC (respiratory chain) via DHODH, impairment of DHODH should affect the RC function. To investigate this, we used siRNA (small interfering RNA)-mediated knockdown and observed that DHODH knockdown induced cell growth retardation because of G_2/M cell-cycle arrest, whereas pyrimidine deficiency usually causes G_1/S arrest. Inconsistent with this, the cell retardation was not rescued by exogenous uridine, which should bypass the DHODH reaction for pyrimidine synthesis. DHODH depletion partially inhibited the RC complex III, decreased the mitochondrial membrane potential, and increased the generation of ROS (reactive oxygen species). We observed that DHODH physically interacts with respiratory complexes II and III by IP (immunoprecipitation) and BN (blue native)/SDS/PAGE analysis. Considering that pyrimidine deficiency alone does not induce craniofacial dysmorphism, the DHODH mutations may contribute to the Miller syndrome in part through somehow altered mitochondrial function.

Key words: dihydro-orotate dehydrogenase (DHODH), Miller syndrome, mitochondrial dysfunction, pyrimidine pathway, ubiquinone.

Cite this article as: Fang, J., Uchiumi, T., Yagi, M., Matsumoto, S., Amamoto, R., Takazaki, S., Yamaza, H., Nonaka, K. and Kang, D. (2013) Dihydro-orotate dehydrogenase is physically associated with the respiratory complex and its loss leads to mitochondrial dysfunction. Biosci. Rep. **33**(2), art:e00021.doi:10.1042/BSR20120097

INTRODUCTION

Mitochondria are essential organelles that are present in virtually all eukaryotic cells and have fundamental functions in energy production and other metabolic pathways. Mitochondria also participate in calcium and iron storage as well as having important functions in signalling, cell death, cell differentiation and the control of cell cycle and cell growth [1]. Previous studies have shown that mitochondrial dysfunction is responsible for a wide range of human diseases, and mitochondria have a possible relationship with aging [2,3]. Given that the most of ATP production depends on the RC (respiratory chain), maintenance of the mitochondrial genome is critical for individuals to maintain normal health [4,5].

OXPHOS (oxidative phosphorylation) is carried out by >150 structural and enzymatic proteins, which are embedded within the inner mitochondrial membrane and organized into five functional RC complexes: I–V. The 13 mtDNA (mitochondrial DNA)-encoded polypeptides are integral parts of the four mitochondrial RC complexes (I, III, IV and V). Complex II is the only RC complex that lacks mtDNA-encoded subunits [6,7].

Pyrimidine nucleotides are synthesized through two pathways: the *de novo* synthesis pathway and the salvage pathway. The

Abbreviations used: BN, Blue native; CCCP, carbonyl cyanide *m*-chlorophenylhydrazone; COX, cytochrome *c* oxidase; 2D, two-dimensional; DCF, 2′7′-dichlorofluorescein; DCFH-DA, 2′7′-dichlorodihydrofluorescein diacetate; DCPIP, 2,6-dichlorophenol-indophenol; DHO, dihydro-orotate; DHODH, dihydro-orotate dehydrogenase; DMEM, Dulbecco's modified Eagle's medium; DOX, doxycycline; FBS, fetal bovine serum; HA, haemagglutinin; IgG, immunoglobulin G; IP, immunoprecipitation; LFN, leflunomide; mtDNA, mitochondrial DNA; OXPHOS, oxidative phosphorylation; RC, respiratory chain; ROS, reactive oxygen species; SDHA, succinate dehydrogenase complex subunit A; siRNA, small interfering RNA; TFAM, mitochondrial transcription factor A; UMP, uridine monophosphate; UMPS, UMP synthase.

[1] To whom correspondence should be addressed (email uchiumi@cclm.med.kyushu-u.ac.jp).

enzyme DHODH (dihydro-orotate dehydrogenase) catalyses the fourth step in the *de novo* biosynthesis of pyrimidine by converting DHO (dihydro-orotate) into orotate [8,9]. DHODH that is located on the inner membrane of mitochondria is the only enzyme of this pyrimidine biosynthesis pathway, whereas all of the other enzymes are located within the cytosol. DHODH catalyses oxidation of DHO into orotate by transferring electrons to the respiratory molecule ubiquinone through an enzyme-bound redox cofactor, FMN [10]. Thus DHODH relies on ubiquinone, thereby forming a functional link between the mitochondrial RC and pyrimidine biosynthesis.

DHODH has two binding sites. The substrate DHO binds to the first site and is oxidized via a cosubstrate electron acceptor. After the release of orotate, ubiquinone binds to a second site and receives an electron from the cosubstrate. The orotate synthesized by DHODH is converted into UMP (uridine monophosphate) by the enzyme complex UMPS (UMP synthase) [11,12]. DHODH function requires active complex III of the RC [11]: treatment with antimycin A, which is an inhibitor of complex III, reduced DHODH activity and pyrimidine synthesis [13], suggesting that DHODH is functionally linked to complex III activity.

Miller syndrome is a type of acrofacial dysostosis, also known as Wildervanck–Smith syndrome. Its clinical features consist of severe micrognathia, cleft lip and/or palate, hypoplasia or aplasia of the postaxial elements of the limbs, coloboma of the eyelids and supernumerary nipples [14,15]. The mutant gene responsible for the disorder has been found to be *DHODH*, which is located at chromosome 16q22 [16]. In total, 13 mutations from exon 2 to exon 9 in the *DHODH* gene have been reported in Miller syndrome [16,17]. Previously, we identified that the G202A and R346W mutations cause deficient protein stability, and the R135C mutation does not affect stability, but impairs the substrate-induced enzymatic activity, suggesting that impairment of DHODH activity is linked to the Miller syndrome phenotype [18].

In mice, use of the DHODH inhibitor LFN (leflunomide) during pregnancy causes a wide range of limb and craniofacial defects, the most common of which are exencephaly, cleft palate and failure of the eyelid to close [19]. Thus the evidence that *DHODH* mutations cause Miller syndrome reveals a new role for DHODH in craniofacial and limb development that remains to be explored. Considering the unique physical location of DHODH within mitochondria, in the present study, we focused on the function of DHODH in the mitochondrial RC and the cellular effects of its depletion and mutation.

The individual OXPHOS protein complexes I–V specifically interact and form defined supramolecular structures, the so-called respiratory supercomplexes, including interactions among complexes I–III and supercomplexes ($I_1III_2IV_1$ and $I_1III_2IV_2$) [20,21]. It has been reported that DHODH is a single subunit non-proton-pumping oxidoreductase, which reduces ubiquinone [22]. However, there have been no investigations on the association of DHODH with the mitochondrial RC complex at mitochondria.

To explore the role of DHODH in mitochondria, we examined mitochondrial functions such as respiratory complex activity, membrane potential and ROS (reactive oxygen species) production by siRNA (small interfering RNA)-mediated DHODH depletion. Taken together, we propose that DHODH, which resides in the mitochondrial intermembrane space, plays an important role in maintaining the mitochondrial RC through physical association with the respiratory complex. We observed that DHODH plays an important role in Miller syndrome, as well as in mitochondrial-mediated cell viability.

EXPERIMENTAL

Antibodies and chemicals

Anti-DHODH, anti-HA (haemagglutinin) and anti-TFAM (mitochondrial transcription factor A) antibodies were raised in our own laboratory. Anti-p53 (DO-1) was purchased from Santa Cruz Biotechnology. Antibodies against NDUFA8 and NDUFA9 (complex I subunits), SDHA [succinate dehydrogenase complex subunit A (a complex II subunit)], UQCRFS1 (a complex III subunit), COX (cytochrome *c* oxidase) I, II, III (complex IV subunits) and COXVa (complex IV subunit Va) were purchased from Invitrogen. Anti-β-actin and L-DHO were purchased from Sigma. MitoTracker Red and DCFH-DA (2′7′-dichlorodihydrofluorescein diacetate) were purchased from Invitrogen.

Cell culture

Human cervical cancer HeLa cells were cultured in DMEM (Dulbecco's modified Eagle's medium) (Sigma) with 10 % (v/v) heat-inactivated FBS (fetal bovine serum). Cell lines were maintained in a 5 % (v/v) CO_2 atmosphere at 37 °C. In some experiments for uridine supplementation, glucose-free DMEM was supplemented with dialysed FBS (Invitrogen).

Knockdown using siRNAs

The following 25-bp double-stranded *DHODH* siRNAs were generated by Stealth Select RNAi (RNA interference) (Invitrogen): 5′-AUU UAU GGC CCA GAA CUC UCA CUU C-3′ and 5′-GAA GUG AGA GUU CUG GGC CAU AAA U-3′ as *DHODH* siRNA-1; 5′-AUA CCU GUU AAU GAC AGC UUG GUC C-3′ and 5′-GGA CCA AGC UGU CAU UAA CAG GUA U-3′ as *DHODH* siRNA-2. siRNA transfections were performed according to the manufacturer's instructions (Invitrogen). Briefly, 2.5 μl of Oligofectamine™ (Invitrogen) was diluted in 100 μl of Opti-MEM I medium (Invitrogen) and incubated for 5 min at room temperature (25 °C). Next, 25 pmol of DHODH or control duplex Stealth RNA (Invitrogen) in 100 μl of Opti-MEM I were added gently and incubated for 20 min at room temperature. Oligomer–Oligofectamine™ complexes and aliquots of 2×10^5 HeLa cells in 2 ml of culture medium were combined and incubated for 5 min at room temperature. The cells were seeded in six-well dishes with 2 ml of culture medium and assayed at the indicated time by Western blotting and FACS.

Expression constructs

An expression construct containing the *DHODH* cDNA was generated by standard methods. cDNAs of wild-type and mutant *DHODH* were cloned into the BamHI/XhoI sites of the expression vector pcDNA3 (Invitrogen). A *DHODH* cDNA containing the deduced first methionine site was amplified from a cDNA library of human HeLa cells by PCR using the primer set: 5′-CAG AGT CTT CTG CCT CCC TG-3′ and 5′-CAG GGA GGC AGA AGA CTC TG-3′. Then, BamHI and XhoI sites were added to the 5′- and 3′-terminals respectively of the cDNA by a second PCR using the primers 5′-GGA TCC ATG GCG TGG AGA CAC CTG AAA AAG C-3′ and 5′-CTC GAG TCA CCT CCG ATG ATC TGC TCC-3′. The PCR product was digested with BamHI and XhoI. The DNA fragment encoding DHODH, a DNA fragment encoding an HA-tag and a pcDNA5/FRT vector (Invitrogen) were digested with BamHI and XhoI and ligated together. The vector was named pDHODH-HA.

Cell proliferation assay

To determine cell proliferation, HeLa cells transfected with control- or both *DHODH* siRNAs were seeded in 24-well plates at a density of 1×10^4 cells per well. Cells (1×10^4) were seeded in triplicate in 35-mm dishes and cultured in dialysed 10% (v/v) FBS (Invitrogen). Cells were trypsinized and counted daily for up to 96 h using a Coulter Counter (Beckman Coulter). Uridine (1 mM) was added on day 0.

Immunoblotting

HeLa cells were lysed in TNE lysis buffer (50 mM Tris/HCl, pH 7.5, 1 mM EDTA, 150 mM NaCl and 0.5% Nonidet P40) and proteins (20 μg) were separated by SDS/PAGE and immunoblotted with the indicated specific antibodies. The signals were visualized with HRP (horseradish peroxidase)-labelled anti-rabbit IgG (immunoglobulin G) and an ECL® (enhanced chemiluminescence) reagent (GE Healthcare). The chemiluminescence was recorded and quantified with a chilled CCD (charge-coupled-device) camera (LAS1000plus; Fuji Photo Film).

Cell-cycle analysis

siRNA-transfected HeLa cells were trypsinized and collected by centrifugation, washed and resuspended in 0.1% BSA plus PBS and fixed in 70% (v/v) ethanol at a density of 1×10^6 cells/ml. After the addition of 1000 units of RNase A and a 15-min incubation at room temperature, the cells were stained with 10 μl of propidium iodide for 1 h. The cell cycle was analysed by flow cytometry with an FACSCalibur™ instrument (Becton Dickinson). The data were analysed using FlowJo software (Tree Star).

Analysis of ROS production

The intracellular H_2O_2 concentration was estimated by means of an oxidation-sensitive fluorescent probe dye, DCFH-DA (Invitrogen). DCFH-DA is deacetylated intracellularly by non-specific esterases, then further oxidized by cellular peroxides to the fluorescent compound DCF (2′7′-dichlorofluorescein). In brief, cells were incubated with the *DHODH* or control siRNA(s) for 72 h. Then cells were washed in PBS and incubated with 20 mM DCFH-DA at 37 °C for 30 min according to the manufacturer's instructions. DCF fluorescence was detected using FACSCalibur™ flow cytometry (Becton Dickinson). For each sample, 10 000 events were monitored. H_2O_2 production was expressed as mean fluorescence intensity, which was calculated by FlowJo software.

Measurement of mitochondrial membrane potential

Mitochondrial membrane potential ($\Delta\psi$m) was estimated using a JC-1 probe (Invitrogen). This reagent is a highly reliable, cationic and mitochondria-specific fluorescent dye, which becomes concentrated in mitochondria in proportion to the $\Delta\psi$m, because it is highly lipophilic. Increasing amounts of dye accumulate in mitochondria with increasing $\Delta\psi$m and ATP-generating capacity. The dye is present as monomers at lower concentrations (green fluorescence), but at higher concentrations forms J-aggregates (red fluorescence). The ratio of the fluorescence at 590 nm to that at 527 nm represents the relative $\Delta\psi$m value. A 10 μM concentration of CCCP (carbonyl cyanide *m*-chlorophenylhydrazone) was used as a control experiment, which collapses the mitochondrial membrane potential. Fluorescence was measured at the two wavelengths by an FACSCalibur™ instrument (Becton Dickinson).

Cross-linking and IP (immunoprecipitation) using anti-HA antibodies

Each step was carried out at 4 °C or on ice. DOX (doxycycline)-induced HeLa (DHODH–HA-expressing) cells (1×10^8 cells) were homogenized with a Potter–Elvehjem homogenizer in 2 ml of homogenizing buffer (10 mM Hepes/KOH, pH 7.4, 0.25 M sucrose and 1 mM EDTA) and centrifuged at 900 ***g*** for 10 min. The supernatant (about 2 ml) was diluted with 2 ml of 20% Percoll buffer [0.25 M sucrose, 20 mM Tris/HCl, pH 7.4, 1 mM EDTA and 20% Percoll (GE Healthcare)], and the sample was overlaid on a discontinuous Percoll density gradient (4 ml of 40% and 4 ml of 20% Percoll buffer) in a 12-ml centrifugation tube. After centrifugation at 24 000 rev./min for 1 h using a SW41Ti rotor (Beckman Coulter), the mitochondrial band, located in the middle of the tube, was removed.

Mitochondrial protein (2 mg) was suspended in 1 ml of cross-linking buffer (0.25 M sucrose, 20 mM Hepes/KOH, pH 7.4, 2 mM EDTA and 25 mM NaCl). Then, 27 μl of 37% (v/v) formaldehyde or distilled water (as a control) were added and the mixture was kept on ice for 2 h. After incubation, 125 μl of 1 M glycine was added to quench the cross-linking reaction, and the sample was centrifuged at 10 000 ***g*** for 1 min to precipitate the mitochondria. The mitochondria were solubilized with 100 μl of IP buffer (10 mM Tris/HCl, pH 7.4, 150 mM NaCl, 1 mM EDTA, 0.5% BSA and 0.5% Nonidet P40) containing 40 μl of beads coated with anti-HA antibodies and control mouse IgG. After a 12-h rotation, the beads were washed four times with wash buffer

(IP buffer without BSA) and eluted with 1 M glycine (pH 2). The immunoprecipitates were heated at 95 °C for 30 min to cleave the cross-links and the proteins were separated by SDS/PAGE (12 % gels) and immunoblotted with each antibody.

BN (Blue native)-PAGE

Mitochondrial protein was prepared by the method described above. A 1 ml aliquot of 4×BN sample buffer consisting of 1.5 M 6-aminohexanoic acid, 0.05 M Bis-Tris, pH 7.0, 65 μl of 10 % *n*-D-maltoside, 20 μl of proteinase inhibitor mixture (Roche) and 100 μl of glycerol. BN sample buffer (2.5 μl of 4×buffer) was mixed with 10 μl of each sample (5–10 μg of mitochondrial protein) and loaded on to a 3–12 % BN–PAGE gradient gel (Invitrogen). Electrophoresis was performed using a commercial system (Invitrogen) with 200 ml of cathode buffer in the upper (inner) buffer chamber and 150 ml of anode buffer in the lower (outer) buffer chamber. The cathode buffer was prepared from a 20×stock: 500 mM Tricine, 150 mM Bis-Tris, pH 7.0 and 0.02 % (w/v) Serva Blue 27 G-250, supplemented with 0.02 % *n*-D-maltoside. The 1×anode buffer consisted of 50 mM Bis-Tris, pH 7.0. Electrophoresis was carried out at 4 °C at 80 V for 1 h and then raised to 150 V for 1.5 h. The separated proteins were transferred electrophoretically on to a PVDF membrane and immunoblotted.

After BN gel electrophoresis, the gels were further processed for 2D (two-dimensional) SDS/PAGE analysis. After electrophoresis, the gels were electroblotted on to Hybond-P PVDF membranes (Amersham) and sequentially probed with specific antibodies.

Biochemical assay of RC activity

DHODH-dependent and respiratory enzymatic activities were measured by spectrophotometry (U-3210; Hitachi). Stable DHODH-expressing HeLa cells were lysed in a hypotonic buffer (2.5 mM Tris/HCl, pH 7.5 and 2.5 mM $MgCl_2$) on ice for 15 min, and then sonicated for 15 s (25 % output, duty cycle; TAITEC Corporation) to measure respiratory complex activity.

The standard reaction buffer contained 50 mM potassium phosphate, 5 mg/ml BSA and 2.5 mM $MgCl_2$. The substrates (electron donors and electron acceptors) varied depending on the assayed complex. Each reaction was terminated by adding a complex-specific inhibitor. The protein concentration for each reaction was measured by BCA (bicinchoninic acid) protein assay (Thermo Scientific). The activities of each complex were indicated by the rate of substrate oxidation or reduction as $nM \cdot min^{-1} \cdot mg^{-1}$ of protein. Each complex was assayed in the presence of inhibitors of the other complexes to ensure that the activity reflected only the enzyme complex of interest.

DHO–ubiquinone oxidoreductase activity

DHODH activity was determined spectrophotometrically at 37 °C by monitoring the decrease in absorbance at 600 nm of reduced DCPIP (2,6-dichlorophenol-indophenol; used as an artificial electron acceptor). Briefly, the reaction was initiated with 20 mM DHO in 1 ml of standard reaction buffer supplemented with 50 μM DCPIP, 2 μg of rotenone (a complex I inhibitor), 2 μg of antimycin A (a complex III inhibitor), 5 mM NaN_3 (a complex IV inhibitor) and 0.1 mg of whole-cell lysate. The data were expressed as $nmol \cdot min^{-1} \cdot \mu g^{-1}$ of protein. The reaction was stopped by the addition of 2 μg of LFN.

Succinate dehydrogenase (complex II) activity

Succinate dehydrogenase (complex II) activity was determined spectrophotometrically at 37 °C. Briefly, the reaction was initiated with 50 μM DCPIP in 1 ml of standard reaction buffer supplemented with 20 mM succinate, 2 μg of rotenone, 2 μg of antimycin A, 5 mM NaN_3 and 0.1 mg of whole-cell lysate. The data were expressed as $nmol \cdot min^{-1} \cdot \mu g^{-1}$ of protein.

Cytochrome c reductase (complex III) activity

Cytochrome *c* reductase (complex III) activity was evaluated spectrophotometrically at 37 °C by monitoring the increase in absorbance at 550 nm of cytochrome *c*. Briefly, the reaction was initiated by the addition of 5 mM decylubiquinone to 1 ml of standard reaction buffer supplemented with 2 μg of rotenone, 5 mM NaN_3, 60 μM cytochrome *c* and 0.1 mg of whole-cell lysate. The reaction was stopped by the addition of 2 μg antimycin A. These data were expressed as $nmol \cdot min^{-1} \cdot \mu g^{-1}$ of protein.

DHO:cytochrome c oxidoreductase activity

DHO:cytochrome *c* oxidoreductase activity was evaluated similarly to cytochrome *c* reductase activity. The assay was conducted under conditions similar to those for complex III, but using 20 mM DHO as the donor substrate and stopping the reaction with 2 μg of antimycin A. Each data point was recorded in triplicate on a single measurement day.

Statistical analysis

Statistical comparisons between groups were analysed by the Student's *t* test or where appropriate, the paired Student's *t* test. Significance was determined for all the data,*$P < 0.05$ and **$P < 0.01$.

RESULTS

siRNA-mediated knockdown of DHODH

DHODH is a key player in the pyrimidine *de novo* biosynthesis pathway and is coupled to the mitochondrial RC [23]. Since DHODH localizes in the inner mitochondrial membrane, we hypothesized that suppression of DHODH expression would affect cell growth and mitochondrial function. To examine the function of human DHODH, we down-regulated the DHODH expression by siRNA-mediated knockdown. The expression of DHODH was diminished by two different *DHODH*-targeting 72-h siRNA treatments (Figure 1A). SDHA (complex II), NDUFA9 (complex I), complex III subunit core I, complex Va (complex V), p53 and β-actin were not affected by *DHODH* siRNA treatment for 72 h

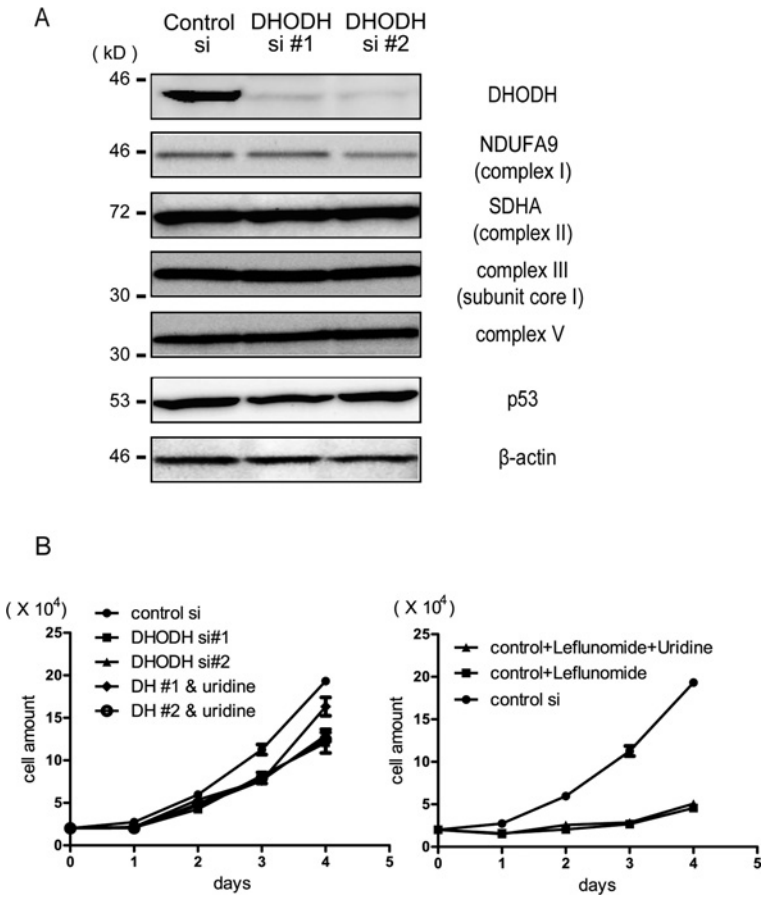

Figure 1 Effects of siRNA-mediated knockdown of DHODH

(**A**) HeLa cells were transfected with control siRNA or two independent *DHODH* siRNAs, #1 and #2, using Oligofectamine™. At 3 days after the transfection, the cells were lysed and immunoblotted with antibodies against DHODH, NDUFA9 (complex I), SDHA (complex II), complex III subunit core I, complex V, p53 and β-actin. (**B**) Depletion of DHODH causes growth retardation. The proliferation rate of siRNA-transfected HeLa cells is shown. HeLa cells were transfected with control or two independent *DHODH* siRNAs on day 0. At the indicated time, the cells were harvested and counted using a cell counter. Left-hand panel, lines represent control siRNA, *DHODH* siRNA #1 and *DHODH* siRNA #2 respectively. Uridine (1 mM) was added on day 0 and day 2 to DHODH-depleted HeLa cells. The cell number was counted at the indicated time after seeding. Right-panel panel, proliferation rate of LFN-treated HeLa cells. HeLa cells were treated with 1 mM LFN on day 0. Uridine was added on day 0 and day 2.

(Figure 1A). A non-targeting siRNA (control siRNA) was used to confirm specificity.

Cell growth retardation

To assess the overall cellular effect of DHODH ablation on cell viability, we closely examined the growth rate. The number of living cells during each siRNA treatment was monitored using a cell counter (Figure 1B). Slight growth retardation was observed in *DHODH* siRNA-treated cells compared with control siRNA-treated cells. To avoid the effect of pyrimidine nucleoside pool deficiency, we added exogenous uridine to the culture medium of the siRNA-treated cells, but this did not prevent the cell growth retardation (Figure 1B).

Recent studies have focused on the ability of the DHODH inhibitor LFN to inhibit the proliferation of a variety of human malignancies such as colon cancer. Therefore we also examined cell growth in the presence of LFN. LFN inhibited HeLa cell proliferation, and as before, exogenous uridine did not rescue the deficit (Figure 1B).

Depletion of DHODH induces G_2/M cell-cycle arrest

To explore the nature of the slowed proliferation due to DHODH depletion, we examined the cell-cycle profile of HeLa cells using flow cytometry. The G_2/M population increased from 5 % in controls to 11 % upon DHODH depletion, suggesting increased cell death (Figure 2), whereas the percentage of cells in G_1- or S-phase rather decreased, although only slightly. Supplementation with uridine did not prevent the G_2/M cell-cycle arrest (Figure 2), suggesting that it was not caused directly by a deficiency in pyrimidine synthesis. These results show that DHODH depletion inhibits HeLa cell proliferation owing to a block in

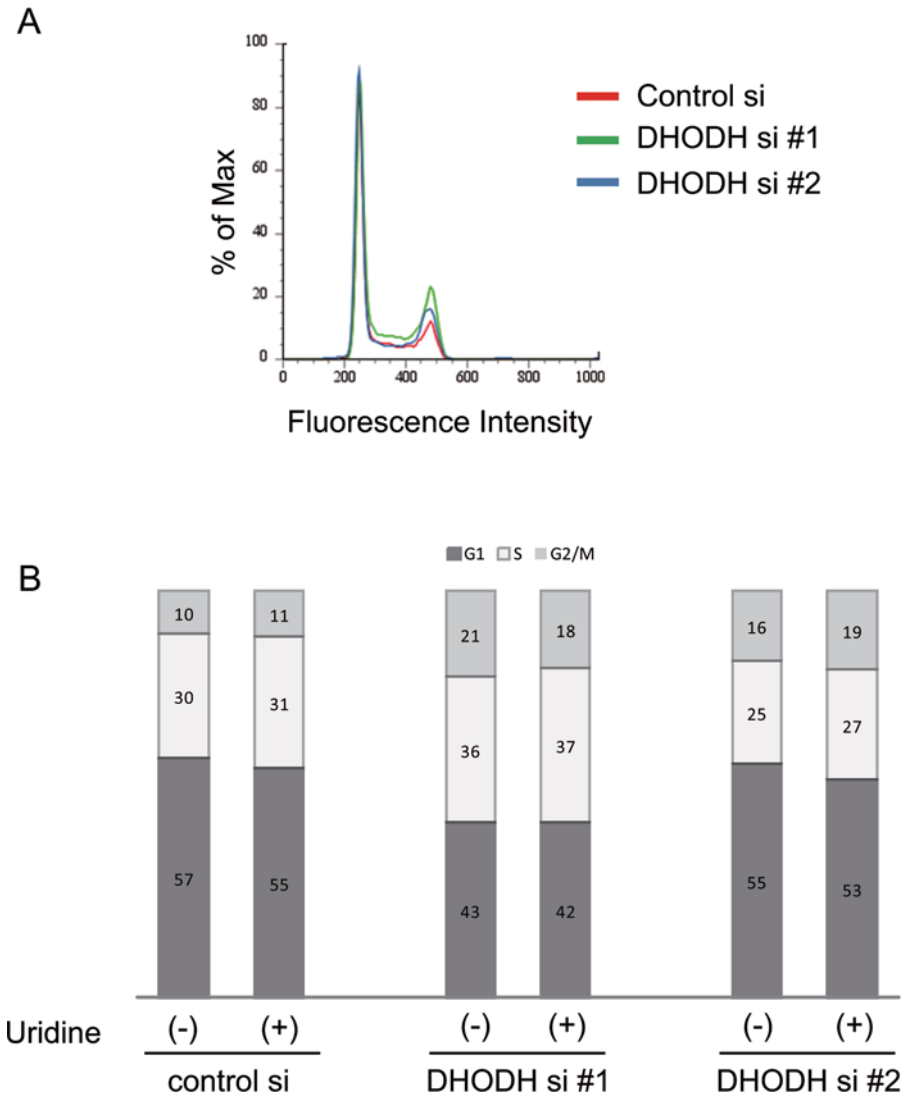

Figure 2 Cell-cycle analysis after DHODH depletion

(**A**, **B**) At 72 h after *DHODH* siRNA transfection, cells were fixed and stained with propidium iodide. Then, the DNA content was measured by flow cytometry. Three separate experiments were carried out, all of which exhibited similar trends. The results of one representative experiment are shown. The cell-cycle phase distribution in each condition is shown as the percentage of cells present in the G_1-, S- or G_2/M-phases.

progression from G_2/M but not to impaired DNA synthesis caused by a pyrimidine deficiency.

Depletion of DHODH is reported to trigger a p53 response because of the deficiency in pyrimidine [13]. The strong expression of p53 by specific inhibition of mitochondrial complex III is attributed to inhibition of DHODH [13]. Since p53 is involved in cell growth and apoptosis, we tested the expression level of p53 in DHODH-knockdown cells; no differences were found among the groups (Figure 1A).

Thus the results of the present study indicated that DHODH is important for normal cell growth in HeLa cells and that there is also another pathway through which DHODH depletion can cause the cell growth retardation and cell-cycle arrest in a manner independent of pyrimidine deficiency or p53 induction.

Depletion of DHODH reduces DHO-dependent reductase activities

During pyrimidine synthesis, DHO is stereospecifically oxidized to orotate, while the prosthetic FMN group is reduced. After dissociation of orotate from the enzyme, $FMNH_2$ is regenerated by a ubiquinone molecule, which is recruited from the inner mitochondrial membrane. We measured the DHO-dependent ubiquinone reductase activity to assess the DHODH enzymatic activity. The ubiquinone reductase activity was completely stopped by LFN, which binds to the substrate-binding site of DHODH (results not shown). DHO-dependent ubiquinone reductase activity was completely inhibited by DHODH depletion by two independent siRNAs (Figure 3A).

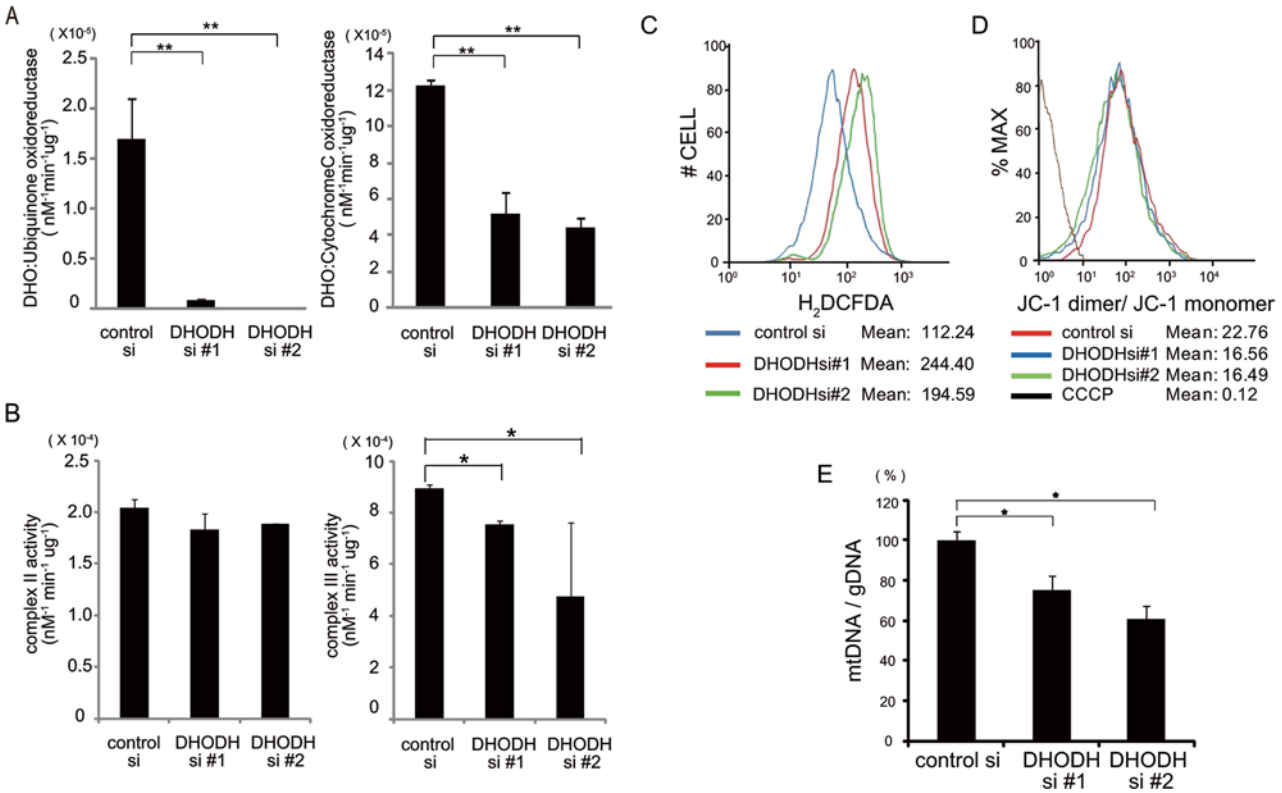

Figure 3 **Depletion of DHODH causes mitochondrial dysfunction**

(**A**) Reduced mitochondrial respiratory activities in *DHODH* siRNA-treated HeLa cells. DHO-ubiquinone oxidoreductase activity and DHO-cytochrome *c* oxidoreductase activity were measured using cell lysates as described in the Experimental section. Reduced enzymatic activities of mitochondrial DHO-dependent oxidoreductase were observed in siRNA-treated cells. The results represent the means ± S.D. of three independent experiments. $^{**}P < 0.01$ against controls. (**B**) Reduced complex III activity after *DHODH* siRNA-mediated depletion in HeLa cells. The activity of each complex (II and III) was measured using cell lysates as described in the Experimental section. Reduced enzymatic activity of mitochondrial complex III was observed in siRNA-treated cells. $^{*}P < 0.05$ against controls. (**C**) Increased ROS production by *DHODH* siRNA-mediated knockdown. HeLa cells were transfected with control (green) or the two independent *DHODH* siRNAs #1 and #2 (red). After 72 h, the cells were treated with 10 μM DCFH-DA for 30 min and were subjected to FACS for quantitative estimation of ROS. (**D**) Decreased mitochondrial membrane potential in DHODH-depleted HeLa cells. HeLa cells were stained with the fluorescent dye JC-1 and then analysed by flow cytometry at 488 and 590 nm. The fluorescence ratio of JC-1 dimer (red) to JC-1 monomer (green) is shown. Dissipation of the membrane potential with CCCP was used as a control. (**E**) Reduced mtDNA copy number after DHODH depletion. The amount of mtDNA per cell was estimated based on the ratio of mtDNA/nuclear DNA [ND2/HPRT (hypoxanthine-guanine phosphoribosyltransferase)] by real-time PCR. HeLa cells were treated with control or *DHODH* siRNA for 72 h. The value in control siRNA-treated cells was set at 100% for each gene. $^{*}P < 0.05$.

Next, we measured DHO–cytochrome *c* oxidoreductase activity after depletion of DHODH. The enzymatic activity was inhibited by the addition of antimycin A (results not shown). DHO–cytochrome *c* oxidoreductase activity was also reduced, although more weakly than the DHO-dependent ubiquinone reductase activity, after DHODH depletion (Figure 3A). We confirmed that DHODH activity was reduced by siRNA treatment.

Depletion of DHODH reduces complex III activity partially

As DHODH is coupled to the mitochondrial RC [23], we asked whether DHODH depletion affected the activity of the other respiratory complexes in mitochondria. We measured the activities of the electron transport chain complexes by spectroscopic assays after siRNA-mediated DHODH knockdown. The activity of complex III was slightly reduced after DHODH depletion in HeLa cells, whereas the activities of complexes II were unchanged (Figure 3B). Thus depletion of DHODH affected complex III but not complex II although DHODH physically interacts with both of them, as shown below (see Figure 4).

Depletion of DHODH increases mitochondrial ROS

The level of ROS plays an important role in cell signalling. Since the oxidation of DHO to orotate is linked to the generation of superoxide from mitochondria [24,25], inhibition of DHODH by siRNA may alter the rate of superoxide generation from mitochondria. Therefore we assessed the cellular levels of mitochondrial superoxide by measuring the oxidation-sensitive dye DCFH-DA to examine whether DHODH siRNA-mediated knockdown led to the generation of ROS. After 72 h transfection,

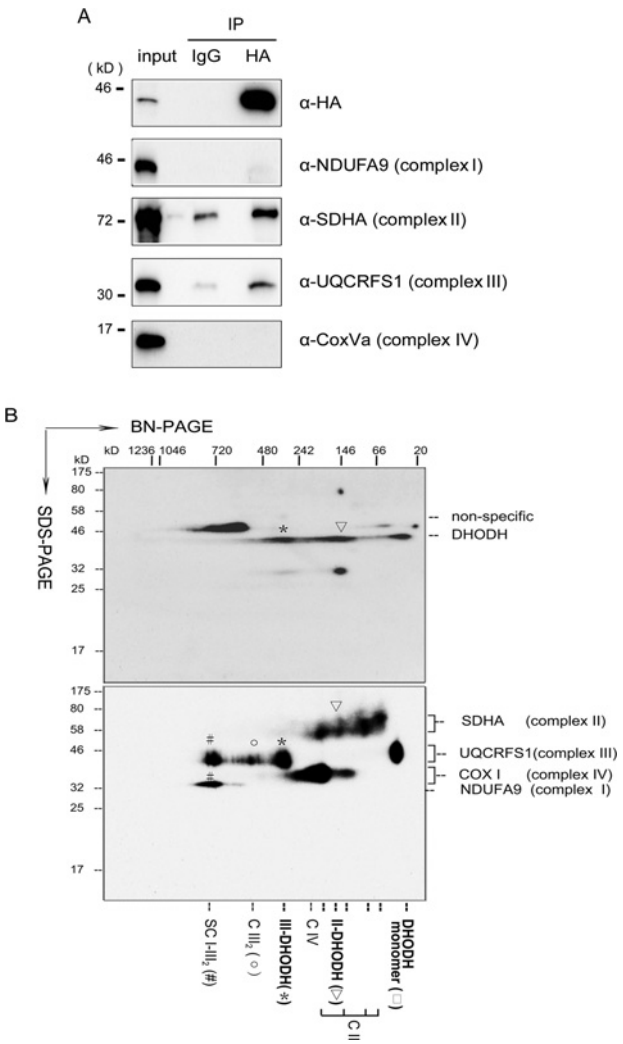

Figure 4 DHODH is associated with complexes II and III

(**A**) DHODH associates with respiratory complexes II and III. DHODH–HA-transfected HeLa cells were treated with DOX for 48 h. The mitochondrial fraction was purified on a Percoll density gradient and lysed with TNE buffer. After cross-linking, immunoprecipitates obtained with anti-HA and mouse IgG antibodies were separated by SDS/PAGE and immunoblotted with anti-HA, NDUFA9 (complex I), SDHA (complex II), UQCRFS1 (complex III) and COXVa (complex IV) antibodies. IP, immunoprecipitate; α, antibody. (**B**) BN/SDS/PAGE analysis. Isolated mitochondria before and after induction by DOX were solubilized by *n*-D-maltoside and protein complexes were first resolved by BN-PAGE (polyacrylamide concentration gradient, 3–12%) and resolved in a second dimension by SDS/PAGE. The transferred proteins were immunoblotted with the indicated antibodies. SC I–III_2, supercomplex formed from complexes I and III_2; $CIII_2$, dimeric complex III; CIV, complex IV; II, succinate dehydrogenase complex II; III_2–DHODH, association with complex III and DHODH; II–DHODH, association with complex II and DHODH. DHODH is shown as monomers. The molecular masses (in kDa) of the molecular mass standards are shown.

we observed a statistically significant increase in fluorescence from the control level (mean: 112.24) to two independent DHODH siRNA levels (mean: 244.4 and 194.6 respectively), indicating that large amounts of free radicals were produced in HeLa cells when DHODH was depleted (Figure 3C).

DHODH siRNA-mediated knockdown reduces mitochondrial membrane potential

A tight link exists between changes in mitochondrial ROS generation and collapse of the $\Delta\psi$m. ROS production is intimately linked to the electrochemical gradient generated by the OXPHOS complexes in mitochondria. The mitochondrial permeability transition has been implicated in $\Delta\psi$m collapse. The $\Delta\psi$m in two independent *DHODH* siRNA transfectants remained at low levels compared with that in control siRNA-transfected cells (Figure 3D). CCCP-treated cells served as a positive control for depolarization of the mitochondrial membrane. Together, these results suggest a role for DHODH in mitochondrial physiology, which can be critical to cell viability.

mtDNA copy number and RNA expression

Oxidative stress can cause mtDNA damage and subsequent loss of mtDNA [26,27]. Considering the localization of DHODH in mitochondria, we examined the effect of DHODH knockdown on mtDNA copy number using real-time PCR. We observed a decline in mtDNA by 30% (Figure 3E). Taken together, the mitochondrial dysfunction and the decline in mtDNA copy number support that DHODH plays a role in mitochondrial function.

DHODH associates with respiratory complexes II and III

The OXPHOS enzyme complexes comprise the RC complexes I, III, IV and V, plus a set of accessory proteins that supply electrons to ubiquinone, including respiratory complex II, the electron-transferring flavoprotein–ubiquinone oxidoreductase and DHODH [28]. It has been proposed that the RC can be viewed as one functional and physical unit called the respirasome; interactions among complexes I–III and supercomplexes ($I_1III_2IV_1$ and $I_1III_2IV_2$) have been reported [20]. Considering the action of DHODH and its dependence on ubiquinone-mediated electron transfer, we hypothesized that DHODH might be involved in forming associations with other complexes.

To test this, we immunoprecipitated DHODH–HA-associated complexes with an anti-HA antibody from DHODH–HA-overexpressing HeLa cells after cross-linking (Figure 4A). Under these conditions, UQCRFS1 (complex III) and SDHA (complex II) were detected in the immunoprecipitates. However, NDUFA9 (complex I) and COXVa (complex IV) were not immunoprecipitated with the anti-HA antibody (Figure 4A). These results suggest that DHODH is closely associated only with respiratory complexes II and III.

DHODH co-migrated with respiratory complexes II and III

To identify the DHODH-associated proteins in complexes II and III, we performed BN-PAGE analysis and 2D gel BN-PAGE–SDS/PAGE analysis. The respiratory complexes and supercomplex bands separated by 2D BN/SDS/PAGE were immunoblotted individually with antisera to components of the respiratory complexes. Variable patterns of staining of the supercomplex and

DHODH bands were observed (Figure 4B). Blotting for DHODH identified the three bands (300, 150 and 40 kDa). Blotting for complex I using NDUFA9 identified the largest band. The two highest relative molecular mass bands (~800 kDa) corresponded to the previously described mobility of the respiratory supercomplexes [29].

Blotting for complex II using SDHA identified four bands about 70–200 kDa, one band of 150 kDa was the same size as DHODH, suggesting that two proteins might co-migrate. Blotting for complex III using UQCRFS1 identified three bands. The largest bands corresponded to supercomplexes I_1–III_2 and I_1–III_2–IV_1, whereas the third band (~400 kDa) was the appropriate size for complex III (III). This third band was same size as DHODH, suggesting that there might be an association between complex III and DHODH.

The IP and BN/SDS/PAGE analysis showed that DHODH is associated with complexes II and III, suggesting that DHODH depletion would partially affect RC activity in mitochondria. Previously, we observed that DHODH depletion reduced complex III activity, suggesting that a physical association with complex III might be important for DHODH function.

DISCUSSION

In higher eukaryotes, pyrimidine biosynthesis is linked to the mitochondrial RC and ATP production at the level of the DHODH enzyme. In the present study, we demonstrated that (i) DHODH knockdown induces cell growth retardation and G_2/M cell-cycle arrest; (ii) this effect is not rescued by the addition of uridine; (iii) depletion of DHODH causes mitochondrial dysfunction such as decreased mitochondrial membrane potential, decreased complex III activity and increased ROS production; (iv) in mitochondria, DHODH is associated with respiratory complexes II and III. We propose that impairment of DHODH activity is linked to mitochondrial dysfunction, contributing at least in part to cell growth retardation, cell-cycle arrest and finally the Miller syndrome phenotype.

Miller syndrome is inherited in an autosomal recessive or compound heterozygous pattern [16]. Miller syndrome disrupts the development of the first and second pharyngeal arches. It remains unclear exactly how *DHODH* gene mutations lead to abnormal development of the pharyngeal arches. It is important to note that DHODH is the fourth of six enzymes in the *de novo* pyrimidine synthesis pathway [10]. The other five enzymes in this pathway constitute two different enzyme complexes located in the cytoplasm. The first three enzymes form the multi-enzyme complex CAD (carbamoyl phosphate synthetase, aspartate transcarbamoylase and dihydro-orotase), and the fifth and sixth enzymes form UMPS.

The neural crest is an important pluripotent cell population that originates in the neural folds. During neurulation, the neural crest cells detach from the neural folds and migrate into the embryo to give rise to numerous structures. Defects in neural crest cell formation, proliferation, migration and/or differentiation are considered responsible for craniofacial abnormalities, which constitute up to one-third of all congenital birth defects [30,31].

White et al. [32] reported that LFN, an inhibitor of DHODH, led to an almost complete abrogation of neural crest development in zebrafish and to a reduction in the self-renewal of mammalian neural crest stem cells. LFN exerts these effects by inhibiting the transcriptional elongation of genes that are required for neural crest development. Particular developmental pathways in neural crest cells have a direct bearing on melanoma formation, suggesting that DHODH is also involved in neural crest cell proliferation and development.

LFN reduces *de novo* pyrimidine biosynthesis by selectively inhibiting DHODH [33]. LFN has been reported to cause multiple malformations when administered to pregnant rats, rabbits or mice, including exencephaly, cleft palate, tail deformities and anomalies of the axial skeleton [19,34].

Many birth defects, such as Miller syndrome and methotrexate-induced embryopathy, are associated with craniofacial malformations. These data suggest that the development of neural crest stem cells is involved in craniofacial malformations [30], and the malformations observed in individuals with Miller syndrome could be caused by failure of correct neural crest cell development because of loss of DHODH function.

ROS have been suggested to play an important role in the aetiology of agent-induced congenital anomalies, including those produced by radiation [35] and thalidomide [36]. Since ROS, which include hydroxyl radicals and superoxide anions, are highly reactive and thus short-lived, mechanistic studies of ROS-induced teratogenicity have benefited from *in vivo* studies. DHODH, an enzyme associated with mitochondrial electron transport [9], could be an important link among mitochondrial bioenergetics, cell proliferation, ROS production and apoptosis in certain cell types.

Depletion of ribonucleotide pools is known to be a strong inducer of the p53 response, which, in normal fibroblasts, results in a p53-dependent arrest at the G_1/S-phase of the cell cycle [37]. We observed that siRNA-mediated depletion of DHODH-induced cell growth retardation and G_2/M arrest in HeLa cells, but did not induce the p53 protein, suggesting that depletion of DHODH can also cause the cell growth retardation in a p53-independent manner. This could be attributed to the tissue-specific variation. Further studies are required to answer this question.

Human DHODH is composed of two domains: a large C-terminal domain (Met^{78}–Arg^{396}) and a smaller N-terminal domain (Met^{30}–Leu^{68}), connected by an extended loop. The large C-terminal domain can be best described as an α/β-barrel-fold with a central barrel of eight parallel β-strands surrounded by eight α-helices. There are some proximal redox sites and ends with several charged or polar side chains (Gln^{47}, Tyr^{356}, Thr^{360} and Arg^{135}). Arg^{135}, which is located at the ubiquinone-binding site, is conserved from human to *Plasmodium falciparum*. We observed that R135C-mutated DHODH, which has been reported in Miller syndrome, showed proper mitochondrial localization but no DHO-dependent enzymatic activity. Since the α- and β-barrel domains of DHODH form a tunnel to the active site of enzymatic activity, compounds interacting with the α- and β-barrel domains

can block DHODH activity. G152R and R346W are located in the α-barrel domains of DHODH; the G152R and R346W mutations would be expected to result in conformational changes that lead to an unstable protein.

Hirano and co-workers [38] reported that subsets of co-enzyme Q10-deficient cells with increased ROS, morphologically abnormal mitochondria and decreased mitochondrial membrane potentials may be shifting to a low mitochondrial energy state and eventual death. The protective effects of antioxidants against superoxide production and cell death support the notion that ROS production triggers cell death. DHODH depletion also resulted in increased ROS production, decreased membrane potential and cell growth retardation. Altered redox states of a very locally limited ubiquinone pool might be involved in these cellular events *in vivo*.

In the present study, we observed, for the first time, that DHODH depletion induces mitochondrial dysfunction and cell-cycle arrest. Since DHODH is important for maintaining neural crest cell development, mitochondrial dysfunction in the neural crest cells might cause the craniofacial malformations in Miller syndrome. We propose that impairment of DHODH activity is linked to mitochondrial dysfunction, leading to cell growth retardation and cell-cycle arrest, finally causing the Miller syndrome phenotype.

AUTHOR CONTRIBUTION

JingXian Fang designed and conducted experiments, analysed data and wrote the paper; Takeshi Uchiumi, Haruyoshi Yamaza and Kazuaki Nonaka designed experiments, analysed data and wrote the paper; Mikako Yagi, Shinya Matsumoto, Shinya Takazaki and Rie Amamoto conducted experiments and analysed data; and Dongchon Kang designed experiments and wrote the paper.

ACKNOWLEDGEMENTS

We acknowledge the technical expertise of the staff of the Support Center for Education and Research, Kyushu University.

FUNDING

This work was supported in part by grants-in-aid for scientific research from the Ministry of Education, Culture, Sports, Science and Technology of Japan [grant numbers 19209019 and 21590337].

REFERENCES

1 McBride, H. M., Neuspiel, M. and Wasiak, S. (2006) Mitochondria: more than just a powerhouse. Curr. Biol. **16**, R551–R560
2 DiMauro, S. and Schon, E. A. (2008) Mitochondrial disorders in the nervous system. Annu. Rev. Neurosci. **31**, 91–123
3 Frenzel, M., Rommelspacher, H., Sugawa, M. D. and Dencher, N. A. (2010) Ageing alters the supramolecular architecture of OxPhos complexes in rat brain cortex. Exp. Gerontol. **45**, 563–572
4 Wallace, D. C. (2010) Mitochondrial DNA mutations in disease and aging. Environ. Mol. Mutagen. **51**, 440–450
5 Tuppen, H. A., Blakely, E. L., Turnbull, D. M. and Taylor, R. W. (2010) Mitochondrial DNA mutations and human disease. Biochim. Biophys. Acta **1797**, 113–128
6 Falkenberg, M., Larsson, N. G. and Gustafsson, C. M. (2007) DNA replication and transcription in mammalian mitochondria. Annu. Rev. Biochem. **76**, 679–699
7 Reinecke, F., Smeitink, J. A. and van der Westhuizen, F. H. (2009) OXPHOS gene expression and control in mitochondrial disorders. Biochim. Biophys. Acta **1792**, 1113–1121
8 Loffler, M., Grein, K., Knecht, W., Klein, A. and Bergjohann, U. (1998) Dihydroorotate dehydrogenase. Profile of a novel target for antiproliferative and immunosuppressive drugs. Adv. Exp. Med. Biol. **431**, 507–513
9 Evans, D. R. and Guy, H. I. (2004) Mammalian pyrimidine biosynthesis: fresh insights into an ancient pathway. J. Biol. Chem. **279**, 33035–33038
10 Rawls, J., Knecht, W., Diekert, K., Lill, R. and Loffler, M. (2000) Requirements for the mitochondrial import and localization of dihydroorotate dehydrogenase. Eur. J. Biochem. **267**, 2079–2087
11 Loffler, M., Jockel, J., Schuster, G. and Becker, C. (1997) Dihydroorotat-ubiquinone oxidoreductase links mitochondria in the biosynthesis of pyrimidine nucleotides. Mol. Cell. Biochem. **174**, 125–129
12 Walse, B., Dufe, V. T., Svensson, B., Fritzson, I., Dahlberg, L., Khairoullina, A., Wellmar, U. and Al-Karadaghi, S. (2008) The structures of human dihydroorotate dehydrogenase with and without inhibitor reveal conformational flexibility in the inhibitor and substrate binding sites. Biochemistry **47**, 8929–8936
13 Khutornenko, A. A., Roudko, V. V., Chernyak, B. V., Vartapetian, A. B., Chumakov, P. M. and Evstafieva, A. G. (2010) Pyrimidine biosynthesis links mitochondrial respiration to the p53 pathway. Proc. Natl. Acad. Sci. U.S.A. **107**, 12828–12833
14 Miller, M., Fineman, R. and Smith, D. W. (1979) Postaxial acrofacial dysostosis syndrome. J. Pediatr. **95**, 970–975
15 Donnai, D., Hughes, H. E. and Winter, R. M. (1987) Postaxial acrofacial dysostosis (Miller) syndrome. J. Med. Genet. **24**, 422–425
16 Ng, S. B., Bigham, A. W., Buckingham, K. J., Hannibal, M. C., McMillin, M. J., Gildersleeve, H. I., Beck, A. E., Tabor, H. K., Cooper, G. M., Mefford, H. C. et al. (2010) Exome sequencing identifies MLL2 mutations as a cause of Kabuki syndrome. Nat. Genet. **42**, 790–793
17 Kinoshita, F., Kondoh, T., Komori, K., Matsui, T., Harada, N., Yanai, A., Fukuda, M., Morifuji, K. and Matsumoto, T. (2011) Miller syndrome with novel dihydroorotate dehydrogenase gene mutations. Pediatr. Int. **53**, 587–591
18 Fang, J. X., Uchiumi, T., Yagi, M., Matsumoto, S., Amamoto, R., Saito, T., Takazaki, S., Yamaza, H., Nonaka, K. and Kang, D. (2012) Protein instability and functional defects caused by mutations of dihydro-orotate dehydrogenase with Miller syndrome patients. Biosci. Rep. **32**, 631–639
19 Fukushima, R., Kanamori, S., Hirashiba, M., Hishikawa, A., Muranaka, R. I., Kaneto, M., Nakamura, K. and Kato, I. (2007) Teratogenicity study of the dihydroorotate-dehydrogenase inhibitor and protein tyrosine kinase inhibitor Leflunomide in mice. Reprod. Toxicol. **24**, 310–316
20 Lenaz, G. and Genova, M. L. (2009) Structural and functional organization of the mitochondrial respiratory chain: a dynamic super-assembly. Int. J. Biochem. Cell Biol. **41**, 1750–1772
21 Stuart, R. A. (2008) Supercomplex organization of the oxidative phosphorylation enzymes in yeast mitochondria. J. Bioenerg. Biomembr. **40**, 411–417
22 Rich, P. R. and Marechal, A. (2010) The mitochondrial respiratory chain. Essays Biochem. **47**, 1–23

23 Ruckemann, K., Fairbanks, L. D., Carrey, E. A., Hawrylowicz, C. M., Richards, D. F., Kirschbaum, B. and Simmonds, H. A. (1998) Leflunomide inhibits pyrimidine *de novo* synthesis in mitogen-stimulated T-lymphocytes from healthy humans. J. Biol. Chem. **273**, 21682–21691
24 Forman, H. J. and Kennedy, J. (1978) Mammalian dihydroorotate dehydrogenase: physical and catalytic properties of the primary enzyme. Arch. Biochem. Biophys. **191**, 23–31
25 Krungkrai, J. (1991) Malarial dihydroorotate dehydrogenase mediates superoxide radical production. Biochem. Int. **24**, 833–839
26 Oka, S., Ohno, M., Tsuchimoto, D., Sakumi, K., Furuichi, M. and Nakabeppu, Y. (2008) Two distinct pathways of cell death triggered by oxidative damage to nuclear and mitochondrial DNAs. EMBO J. **27**, 421–432
27 Shokolenko, I., Venediktova, N., Bochkareva, A., Wilson, G. L. and Alexeyev, M. F. (2009) Oxidative stress induces degradation of mitochondrial DNA. Nucleic Acids Res. **37**, 2539–2548
28 Gattermann, N., Dadak, M., Hofhaus, G., Wulfert, M., Berneburg, M., Loeffler, M. L. and Simmonds, H. A. (2004) Severe impairment of nucleotide synthesis through inhibition of mitochondrial respiration. Nucleosides, Nucleotides Nucleic Acids **23**, 1275–1279
29 Schafer, E., Seelert, H., Reifschneider, N. H., Krause, F., Dencher, N. A. and Vonck, J. (2006) Architecture of active mammalian respiratory chain supercomplexes. J. Biol. Chem. **281**, 15370–15375
30 Minoux, M. and Rijli, F. M. (2010) Molecular mechanisms of cranial neural crest cell migration and patterning in craniofacial development. Development **137**, 2605–2621
31 Jones, N. C. and Trainor, P. A. (2004) The therapeutic potential of stem cells in the treatment of craniofacial abnormalities. Expert Opin. Biol. Ther. **4**, 645–657
32 White, R. M., Cech, J., Ratanasirintrawoot, S., Lin, C. Y., Rahl, P. B., Burke, C. J., Langdon, E., Tomlinson, M. L., Mosher, J., Kaufman, C. et al. (2011) DHODH modulates transcriptional elongation in the neural crest and melanoma. Nature **471**, 518–522
33 Breedveld, F. C. and Dayer, J. M. (2000) Leflunomide: mode of action in the treatment of rheumatoid arthritis. Ann. Rheum. Dis. **59**, 841–849
34 Fukushima, R., Kanamori, S., Hirashiba, M., Hishikawa, A., Muranaka, R., Kaneto, M. and Kitagawa, H. (2009) Inhibiting the teratogenicity of the immunosuppressant leflunomide in mice by supplementation of exogenous uridine. Toxicol. Sci. **108**, 419–426
35 Mandal, G., Wyllie, S., Singh, N., Sundar, S., Fairlamb, A. H. and Chatterjee, M. (2007) Increased levels of thiols protect antimony unresponsive Leishmania donovani field isolates against reactive oxygen species generated by trivalent antimony. Parasitology **134**, 1679–1687
36 Hansen, J. M., Carney, E. W. and Harris, C. (1999) Differential alteration by thalidomide of the glutathione content of rat vs. rabbit conceptuses *in vitro*. Reprod. Toxicol. **13**, 547–554
37 Linke, S. P., Clarkin, K. C., Di Leonardo, A., Tsou, A. and Wahl, G. M. (1996) A reversible, p53-dependent G_0/G_1 cell cycle arrest induced by ribonucleotide depletion in the absence of detectable DNA damage. Genes Dev. **10**, 934–947
38 Quinzii, C. M., Lopez, L. C., Gilkerson, R. W., Dorado, B., Coku, J., Naini, A. B., Lagier-Tourenne, C., Schuelke, M., Salviati, L., Carrozzo, R. et al. (2010) Reactive oxygen species, oxidative stress, and cell death correlate with level of CoQ10 deficiency. FASEB J. **24**, 3733–3743

Received 12 September 2012; accepted 14 November 2012

Published as Immediate Publication 7 December 2012, doi 10.1042/BSR20120097